Ultrafast Melting of Superconductivity in an Iron-Based Superconductor

D. Nevola,[1,†] N. Zaki,[1] J. M. Tranquada,[1] W.-G. Yin,[1] G. D. Gu,[1] Q. Li,[1,2] and P. D. Johnson[1,*]

[1]*Condensed Matter Physics and Materials Science Department,*
Brookhaven National Laboratory, Upton, New York 11973, USA
[2]*Department of Physics and Astronomy, Stony Brook University, Stony Brook, New York 11794-3800, USA*

Intense debate has recently arisen regarding the photoinduced changes to the iron-chalcogenide superconductors, including the enhancement of superconductivity and a metastable state. Here, by employing high-energy resolution, we directly observe the melting of superconductivity on ultrafast timescales. We demonstrate a distinctly nonequilibrium response on short timescales, where the gap fills in prior to the destruction of the superconducting peak, followed by a metastable response. We propose that the former is due to pair phase decoherence and speculate that the latter is due to the increase in double-stripe correlations that are known to compete with superconductivity. Our results add to exciting new developments on the iron-based superconductors, indicating that the photoinduced metastable state possibly competes with superconductivity.

I. INTRODUCTION

The superconducting iron chalcogenides have recently generated considerable interest with the recognition that they bring together superconductivity, topology, and magnetism in a single material [1–3]. Superconductivity and topology offer the possibility of topological superconductivity, which in turn presents a platform for hosting Majorana fermions, which are potentially important in qubit technology [4]. Magnetism and topology, on the other hand, offer a platform for the quantum anomalous Hall effect (QAHE). However, superconductivity and the QAHE represent competing states [5], and it is therefore important that an understanding is obtained of the different phenomena driving the system one way or the other. The $FeSe_{1-x}Te_x$ (FST) phase diagram is complex, with the system displaying superconductivity for $x = 0$ and antiferromagnetism for $x = 1$. At around $x = 0.5$ and higher, the possibility of a topological state existing on the surface has also been predicted [6]. The chiral nature of the latter topological surface state (TSS) has been demonstrated using spin-polarized photoemission in one study [1] and

incident circularly polarized light in another [2]. It has also been shown that for $x > 0.5$ ferromagnetism develops in the surface region with the superconducting transition [7]. The associated time-reversal symmetry breaking results in a gap at the Dirac point in the TSS [3].

There have also been a number of studies of this material using time-resolved pump-probe techniques where the system is pumped out of equilibrium and the pathway back to equilibrium provides further insights into the complex interactions that take place between the electrons and collective modes [8–13].

Such techniques have also been applied to the cuprate superconductors for Fermi-surface wave vectors ranging from the nodal direction to the antinodal direction. In general, these studies show a return to equilibrium via different stages. First, the nonequilibrium state decays via e-e interactions on timescales of the order of 100 femtoseconds, establishing a state with a "pseudo-equilibrium" Fermi-Dirac distribution [14–21]. At longer timescales, of the order of picoseconds, energy is subsequently transferred to the lattice via electron-phonon interactions. Studies have also concluded that with IR excitation, the superconducting gap fills in, rather than closing, due to loss of coherence of the superconducting condensate near the node [18,22], while more exotic behavior due to Mott physics may be present at the antinode [23,24].

Pump-probe studies of the Fe-chalcogenide superconductors show a different behavior. These systems still show the fast electron-electron equilibration, but then the material appears to enter a metastable phase that exists on the order of nanoseconds or longer [12,13,25]. The nature of this metastable behavior has been the topic of considerable

discussion. Photoemission studies have speculated about various behaviors, ranging from light-induced superconductivity [12] to light-induced nematicity [25]. The concept of light-induced or enhanced superconductivity appears to follow the pioneering studies on this subject in a number of materials by Cavalleri and co-workers [26–29]. By the very nature of the experimental probes, these studies have tended to focus on high timing resolution. In the present study, we take a different approach. Acknowledging that the light-induced state is metastable and therefore long-lived, we reduce the timing resolution and push for high-energy resolution in the probe beam. Such an approach offers immediate and important new insights into the metastable state. Not only can we, for the first time, identify the coherent peak associated with the bulk superconductivity in a time-resolved study of this material, but we clearly demonstrate from its transient behavior that the incident IR pulse kills the superconductivity and that it does not recover in the time-scale associated with the metastable phase.

In systems with closely competing quantum states, it is known that an incident IR pulse can push the system from one state to another. In the FST materials, it is well established that two different spin or magnetic configurations exist. The low-temperature superconducting phase is characterized by spin correlations of the single-stripe type [30]. At slightly higher temperatures above 40 K, the material adopts double-stripe spin correlations that do not support superconductivity [31]. Equilibrium studies have suggested that this second phase is closely related to the electron coupling with the A_{1g} phonon mode, which is the out-of-plane oscillation of the chalcogen atoms [32]. Interestingly, the out-of-plane chalcogen position has been theoretically tied to the magnetic phase, supporting the significant role of the electron-A_{1g} phonon coupling in determining the magnetic ground state [33,34]. Similarly, out-of-equilibrium studies have shown that the pump-induced metastable state is distinctly related to the A_{1g} phonon mode, eventually leading to a renormalized chalcogen position [11,13]. This renormalized position shows an increased c-axis lattice constant, consistent with increasing the value of x on the FeSe$_{1-x}$Te$_x$ phase diagram [31]. It is then naturally expected that this metastable state will lead to an associated modification of the superconducting and magnetic behavior. In the present study, we find that superconductivity is not supported in this metastable phase; therefore, we postulate that it reflects a transition from the superconducting single-stripe phase to the double-stripe nonsuperconducting state, driven by photoinduced orbital fluctuations.

II. METHODS

Single crystals were grown using the unidirectional solidification method. The superconducting properties of the single crystals studied here were previously characterized by magnetization measurements, having a superconducting transition temperature T_c of 14.5 K [3].

The time-resolved angle-resolved photoelectron spectroscopy (tr-ARPES) was performed at Brookhaven National Laboratory using a SES-2002 analyzer. The probe pulse was generated using the output of a Coherent Vitara-T/RegA 9050 setup, which consists of 70-fs-long, 800-nm pulses at 250 kHz. A cascade of nonlinear processes was then used to produce the fourth harmonic (200 nm). The fourth harmonic pulses were finally passed through a monochromator before entering the vacuum chamber. The 800-nm fundamental pulses were used to pump the system. The energy and time resolutions were 6.6 meV and 500 fs, respectively. Space charge effects were carefully monitored before each experiment. The temperature-dependent measurements were acquired first at 5 K, then by increasing to 15 K, and finally reproduced again at 5 K on the sample spot, in order to ensure that the effect was reproducible over a full temperature cycle. The results in this paper have been repeated on multiple cleaves.

The fits in Fig. 3(c) consist of the sum of two exponentially modified Gaussians, which is the analytical form for an exponential convolved with a Gaussian. The decay time of the longer one is fixed to be 1 ns in order to mimic the constant offset, and the width of the Gaussian corresponds to the time resolution. The fits in Fig. 3(d) consist of the sum of an error function and the exponentially modified Gaussians, where the widths in both correspond to the resolution and are fixed to be the same.

III. BAND STRUCTURE

We start by reviewing the changes to the band structure near the Γ point through the superconducting transition, schematically shown in Figs. 1(a) and 1(b) [for a more comprehensive understanding of the band structure, the reader is directed to Refs. [1–3], from which the schematics in Figs. 1(a) and 1(b) are derived]. We focus mainly on the three bands closest to the zone center, which is comprised of two bulk bands and a topological surface state. Above T_c, the outermost bulk band forms a hole pocket that crosses E_F near ± 0.15 $\overset{\circ}{A}^{-1}$ [35]. At the zone center is another holelike band that reaches its maximum of about 16 meV below E_F [1–3]. These bulk bands are typically referred to as the α_2 and α_1 bands, respectively. The topological surface state emerges from the top of the α_1 band to form a small, electronlike pocket [1–3]. Recent efforts have demonstrated that the band inversion leading to the TSS results from the combination of spin-orbit effects in the Te atoms and hybridization from the Fe $d_{xz/yz}$ and Te p_z orbitals [6,36]. Theoretical efforts to reproduce the ground-state band structure highlight the role of strong electronic correlations that we believe play a vital role in the metastable behavior observed in tr-ARPES, as will be discussed in more detail later. For example, in one study, density functional theory requires a strong renormalization
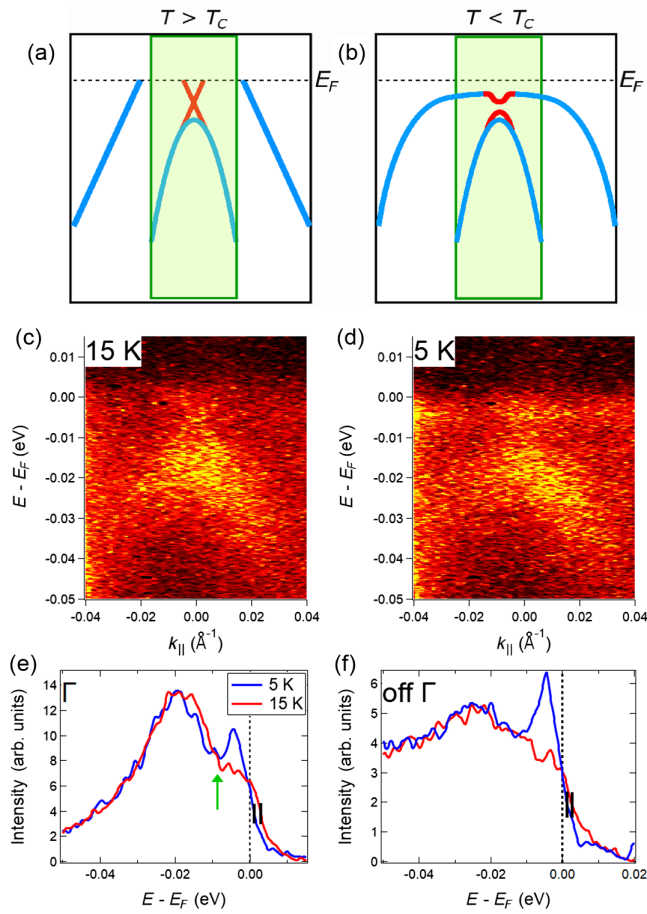
FIG. 1. Band structure of $FeSe_{0.45}Te_{0.55}$. Panels (a) and (b) schematically show the band structures near the Γ point above and below T_c, respectively, and are based on the results in Refs. [1–3]. The bands in blue and red represent bulk and surface contributions. The green box is representative of the angular window probed by the experiment. (c,d) Static ARPES, probed with p-polarized light at 15 K and 5 K. (e,f) Energy distribution curves centered at $k = 0$ and $k = 0.03$ Å. The momentum integration windows are 0.03 Å^{-1} and 0.02 Å^{-1} for panels (e) and (f). Red and blue EDCs represent those at 15 K and 5 K, respectively. The data in panels (e) and (f) have been smoothed for clarity.

to reproduce the experimentally observed energy scales [36], while another study directly shows that the inclusion of magnetic correlations overcomes this discrepancy [35].

The system undergoes several changes upon cooling through the superconducting transition [Fig. 1(b)]. First, superconducting gaps open up in both the bulk and surface Fermi pockets, with values of $2\Delta \sim 4$ and 3.6 meV respectively [1,37]. Additionally, a weakly dispersive superconducting peak (SP) develops in the vicinity of E_F [37–39]. At the same time, a 5-meV gap opens at the Dirac point in the TSS and has been used to associate the onset of superconductivity with the formation of ferromagnetic order [3]. The polarization-dependent matrix elements have proved a useful method for enhancing or

suppressing these bands. For example, s-polarized light enhances the α_1 band and the TSS, whereas p-polarized light enhances the α_2 band and the SP [3,40]. As we will argue later, such a strong polarization dependence of the SP may reflect its sensitivity to orbital fluctuations, which can be strongly altered by even a weak photoexcitation. For the present study, we probe with p-polarized light because we are interested in the pump-induced changes to superconductivity.

IV. RESULTS

Next, we demonstrate the high-energy resolution of the tr-ARPES experimental configuration by showing the static ARPES results above and below T_c, respectively [Figs. 1(c) and 1(d)]. The low-energy scales associated with the bands of interest emphasize the requirement for such resolution. Above T_c, the α_1 band is clearly visible. However, we note that the α_2 band is outside of our momentum window, which is shown schematically by the green rectangles in Figs. 1(a) and 1(b). We also observe the TSS as a weak intensity plateau extending from the top of the α_1 band. This is more clearly seen in the energy distribution curve (EDC) through the Γ point in Fig. 1(e), where the green arrow indicates the Dirac point. Above the Dirac point at 15 K, the plateau corresponding to the TSS is visible. As alluded to earlier and discussed elsewhere, below T_c, two gaps appear in the spectral response, one at the chemical potential associated with superconductivity and one at the Dirac point reflecting time-reversal symmetry breaking. We are unable to clearly resolve the topological gap because a better momentum resolution is required than available in the present study. The superconducting gap is seen by observing the shift of the leading edge midpoints, shown by the black lines in Figs. 1(e) and 1(f), by 2.5 meV [3]. The formation of the superconducting gap results in the development of a peak just below the Fermi level. Finally, there is a subtle shift towards higher binding energy of the α_1 band that occurs in conjunction with the formation of the gap at the Dirac point [Fig. 1(e)]. All of these changes are also made evident when applying the Lucy-Richardson deconvolution algorithm [41] (see Supplemental Material [42]). Having established the ability to resolve the low-energy effects associated with superconductivity, we now turn to the pump-induced modifications to the superconducting band structure.

Figure 2(a) shows the k-integrated changes to the band structure below T_c upon pumping with an infrared laser pulse. Two features are observed that are absent when pumped above T_c [Fig. 2(b)]: (1) an intensity increase just above E_F and (2) a sharp intensity drop just below E_F. As these changes are not observed above the superconducting transition, they must be associated with superconductivity. Examination of the momentum-integrated EDCs in Fig. 2(c) shows that these intensity changes correspond to the filling of the superconducting gap and destruction of the SP,
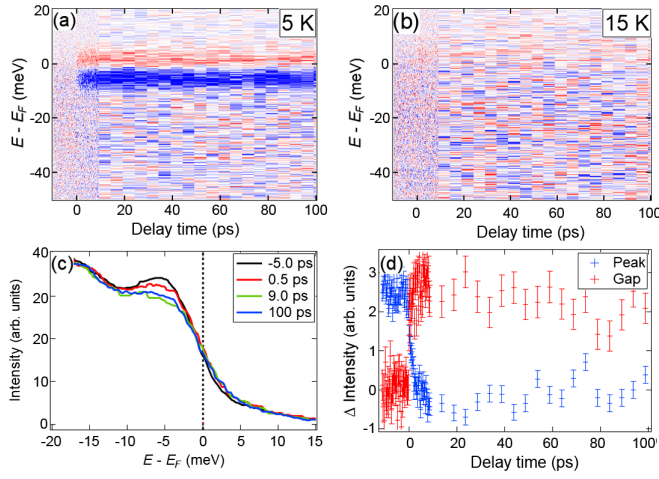
FIG. 2. Photoinduced changes to the k-integrated band structure below (a) and above (b) T_c at an incident pump fluence of 1.2 μJ/cm^2. Red and blue lines indicate an intensity increase and decrease, respectively. (c) Energy distribution curves at various delay times. (d) Intensity dynamics just above and below E_F out to long delay times. The data were averaged over a 7-meV energy range. For clarity, the data below E_F were offset and normalized to match the change above E_F.

FIG. 3. Fluence-dependent dynamics at short delay times. (a) EDCs before (blue line) and after (red line) the pump pulse at 4 μJ/cm^2. (b) Same as panel (a), but with a pump fluence of 2 μJ/cm^2. The dashed black line is the red curve in panel (a), for comparison. (c,d) Dynamics of the momentum-integrated difference images just above (c) and below (d) E_F that correspond to the superconducting gap and quasiparticle peak, respectively. Solid lines correspond to fits.

respectively. These changes are consistent with the static results in Fig. 1 and indicate that superconductivity melts on ultrafast timescales. Identifying the mechanisms responsible for this phenomenon, as well as its recovery, is a novel pathway towards understanding iron-based superconductivity. We now turn to the time dependence for further insight into these processes.

Figure 2(d) shows that after the initial melting of superconductivity, the changes persist up to greater than 100 ps without showing any clear sign of recovery. However, we note that slight deviations from a constant offset after the first few picoseconds can be attributed to noise, a slight drift of the pump beam, or acoustic oscillations that have been observed to occur on these timescales [8]. This is also seen when comparing the k-integrated EDCs at 9 ps to that at 100 ps in Fig. 2(c). Indeed, similar long time behavior has been observed in other optical experiments that have used pump fluences similar to the ones used in this work [8]. This lack of decay on timescales of about 100 ps is intriguing when considering the metastable behavior that has attracted recent interest [12,13,25]. Importantly, the main difference between those studies and the present one is the pump fluence used (much lower in the present case). Furthermore, the linear fluence dependence of the metastable changes with no threshold establishes this long-lived behavior as a derivative of the ground state, meaning that it exists because of the interactions present in the ground state [11]. Thus, the decay bottleneck that is ultimately responsible for the metastable behavior must still be present at the low fluences used in this work. We believe that the reduction of superconductivity is a property of the pump-induced electronic redistribution, and
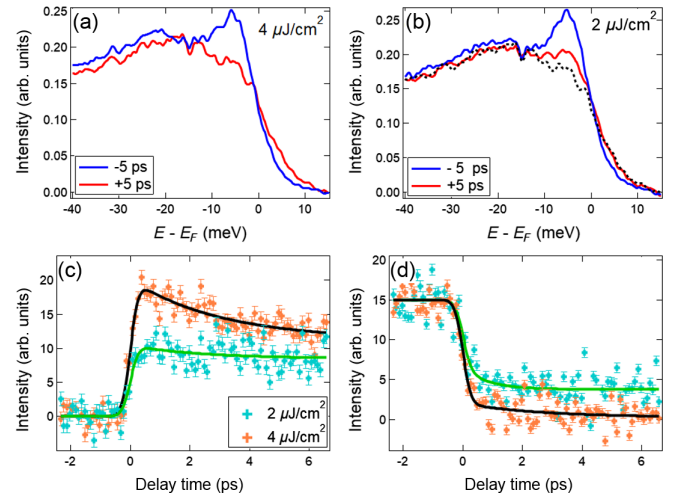
the long-lived behavior results from the same mechanism as the well-reported metastability in FST when pumped at higher fluence [11–13,25]. However, it is also expected that pumping a superconductor at $T < T_c$ naturally leads to the melting of superconductivity on picosecond timescales due to equilibrium heating from the incident laser pulse. The dynamics that we observe at shorter delays do not show the expected picosecond recovery typically associated with lattice heating and must therefore correspond to time-dependent changes to the spectral function, $A(k, \omega, t)$.

We consider the results for two different fluences. Figure 3 shows the dynamics at shorter delays for two different pump fluences. At the higher fluence of 4 μJ/cm^2, the superconducting peak is destroyed, as shown by the difference between the EDCs at negative and positive delay times recorded away from the zone center [Fig. 3(a)]. However, most of the reduction is achieved with the lower fluence of 2 μJ/cm^2 [Fig. 3(c)], which is made clear when comparing the off-Γ EDC at +5 ps (red curve) to the same EDC at 4 μJ/cm^2 (dashed black curve). Comparing the amplitudes at +5 ps for the two fluences allows us to estimate the complete disappearance of the SP at a critical fluence of 3 μJ/cm^2 (assuming a linear dependence on fluence).

Figures 3(c) and 3(d) show the intensity dynamics at the indicated fluences above and below E_F, respectively. Careful analysis of the dynamical data reveals rapid changes equal to the resolution, followed by fluence-dependent picosecond dynamics. The initial change in signal is attributed to a combination of the direct transitions associated with the pump, and subsequent electron-electron interactions that are expected to be reasonably strong in the

iron-based superconductors. Although we are only able to determine an upper bound to this timescale to be 500 fs because of our resolution, reflectivity studies have shown that these initial changes occur within 100 fs [8,9]. At the higher fluence, the positive signal [orange markers in Fig. 3(c)] shows a partial recovery on a timescale of 3 ± 1.5 ps, while the negative signal [orange markers in Fig. 3(d)] shows an initial change equal to the resolution followed by no observable recovery. We interpret the 3-ps timescale as the dissipation of heat into the lattice. However, this same timescale is not observed in the lower fluence, which means that this energy dissipation corresponds to excess heat after superconducting order has melted. Similarly, temperature-dependent reflectivity studies on FST show a similar picosecond timescale that disappears near T_c [8,9].

The dynamics of the SP [Fig. 3(d)] tell a slightly different story. Both fluences probed show no observed recovery on picosecond timescales. With the higher fluence, we expect that we would not observe the reappearance of the SP if there is excess energy after melting superconductivity. This can also be understood in the context of the two-temperature model with a final lattice temperature greater than T_c [43]. If the melting of superconductivity is thermal,

we would observe a recovery of the SP on a timescale of about 3 ps, similar to that above. Furthermore, the recovery would be obvious since the SP is the brightest feature in the difference spectrum in Fig. 2(a) and is particularly sensitive to the temperature in equilibrium. Bonavolanta *et al.* also determined the temperature to only increase by a maximum of 3 K when using a fluence several times those used in this work, making a thermal heating explanation unlikely [9]. Closer examination of the lower fluence data reveals an initial decrease equal to the resolution followed by a further decrease on a timescale of 0.8 ± 0.5 ps. This second timescale suggests that another scattering mechanism is involved in the melting of superconductivity, as will be discussed in the next section. Additionally, since we remain below T_c and observe no recovery of the condensate within the 100-ps measurement window, we conclude that the melting of superconductivity is metastable.

To further emphasize the behavior at short delays, we display the difference EDCs [Fig. 4(a)], which are energy profiles through the data in Fig. 2(a). For the intensity loss, we see an evolution in going from the shortest delay at 0.5 ps to 9 ps. However, for the intensity gain, we do not see the same evolution. After the maximum intensity change is reached within the first 0.5 ps, the intensity remains constant to within the noise level. This means that at short delays, the filling of the gap occurs first on timescales of less than 500 fs.

V. DISCUSSION

The most obvious implication of the results in this work is to demonstrate that superconductivity melts on ultrafast timescales and does not return within the measured time window. This direct demonstration contradicts the conclusions in two recent works that have suggested enhanced superconductivity due to photoexcitation [12,44]. One is an all-optical study that suggests a temporary picosecond enhancement [44], and the other is a tr-ARPES study with lower energy resolution that associates superconductivity with the metastable state [12]. Interestingly, the former study clearly demonstrates nonequilibrium behavior at short delays.

Isoyama *et al.* found an increase in both the real and imaginary parts to the conductivity within the first 1–2 ps, contradicting equilibrium measurements that showed an increase and decrease in the real and imaginary parts to the optical conductivity, respectively, with increasing temperature [44]. Additionally, these changes occur on an energy scale of less than 2 meV, less than the superconducting gap 2Δ, and the same magnitude of the observed leading edge midpoint shift (see Supplemental Material [42]). One possible interpretation is an increase in the size of the condensate, as suggested, but this would manifest as an increased spectral weight within the superconducting peaks on either side of the Fermi level, which we do not observe. Alternatively, we propose the destruction of phase
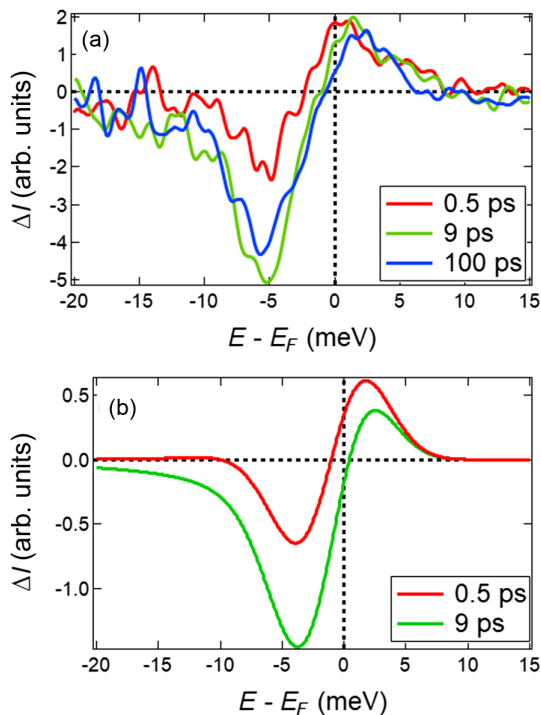

FIG. 4. (a) Time-dependent energy profiles through the data in Fig. 2(a) at delay times of 0.5 ps, 9 ps, and 100 ps. The pump fluence is 1.2 μJ/cm^2. (b) Modeled difference curves as described in the text. The red curve includes only a finite Γ_p, and the green curve includes both a finite Γ_p and decreased spectral function amplitude, as further described in Supplemental Material [42].

coherence among the Cooper pairs caused by their scattering with nonequilibrium bosonic excitations [22]. This mechanism may explain both the increases to the real [45] and imaginary [46] parts of the optical conductivity. It can be modeled by the inclusion of a finite pair scattering rate in the self-energy that describes a superconductor [22,47–49]:

$$\Sigma(\omega) = -i\Gamma_s + \frac{\Delta^2}{\omega + i\Gamma_p}. \tag{1}$$

Here, ω is the energy, Δ is the gap amplitude, Γ_s is the single-particle scattering rate, and Γ_p is the pair scattering rate, indicative of pair scattering with phase fluctuations [22,47]. An increase in Γ_p increases the spectral weight inside the gap, and it was recently found to describe the nonequilibrium changes to the near-nodal spectral function in an optimally doped cuprate [22]. This spectral weight increase inside the gap due to pair phase fluctuations is referred to as a "gap filling," which is not to be confused with the gap closure that typically occurs upon the equilibrium heating of the sample up to T_c. In the former case, pairs remain, so the distance between the two Bogoliubov quasiparticle peaks remains unchanged, but the widths of the peaks increase (albeit asymmetrically favoring the side closer to E_F). In the latter, which is referred to as a "gap closing," Bogoliubov quasiparticle peaks move closer together as a result of the Cooper pairs breaking, and this represents the shrinking of the superconducting gap Δ.

To provide a more quantitative picture, we model the difference curves by using the self-energy in Eq. (1) (see Supplemental Material [42] for more details). First, we show the experimental data at three delay times in Fig. 4(a) [the data correspond to energy profiles at the specified delay times selected from the data in Fig. 2(a)]. The amplitudes of the positive and negative signals are nearly identical in the 0.5-ps (resolution-limited) data, while the negative signal grows on a picosecond timescale and remains constant for more than 100 ps. As shown in Fig. 4(b), including a finite Γ_p (while keeping all other parameters constant) is enough to reproduce the experimental data at 0.5 ps. The data at longer delays were reproduced by reducing the amplitude of the spectral function, which we think resembles the breaking of Cooper pairs. The fact that we are able to reproduce the curve shape at 0.5 ps by including the pair scattering rate, which is a nonequilibrium parameter, supports our hypothesis that pump-induced phase fluctuations reflect electronic correlations.

Before discussing the timescales in detail, we briefly discuss the nature of the photoexcitation. The precise locations in energy and momentum after the pump depend on fine details such as a complete knowledge of the band structure within 1.55 eV of E_F and the matrix elements, which may heavily depend on the orbital components of the bands. Neither of these details is well understood, so we are unable to make any definitive statements about the direct excitations. However, in the most extreme case where the excitations are primarily from E_F to +1.55 eV and at the Γ point (i.e., directly pumping out of the superconducting peak in our experimental window), we expect that the high energy of the absorbed photon is enough to break the Cooper pair and melt superconductivity. If the excitations are made anywhere else in the Brillouin zone (a much more likely scenario), a bath of nonequilibrium bosons is created while the pairs remain. This can cause decoherence amongst the Cooper pairs, and it again results in the melting of superconductivity because the pairs must remain coherent for superconductivity to be present. In any case, we expect nontrivial changes to the electronic structure after pumping because superconductors are many-body systems where small perturbations may cause dramatic effects.

The photoinduced changes that we observed contain three timescales that offer further insight into the microscopic mechanisms responsible for the ultrafast melting of superconductivity. First, the gap filling occurs within our resolution. This suggests that the phase fluctuations are of electronic origin. The fluctuations may be caused by the scattering of Cooper pairs with nonequilibrium bosons [22]. We speculate that these bosons are of the form of magnetic excitations. Second, the persistent decrease in the SP occurs on a picosecond timescale. We attribute this to the breaking of pairs by optical phonons that are generated upon the decay of high-energy quasiparticles. A similar temperature-dependent timescale was observed in time-resolved reflectivity [9] and was also ascribed to phonons. The final timescale is the recovery of the superconducting features, which are longer than our temporal window, indicating that the changes mentioned above are metastable. The key question is *why* they are metastable, for which we offer two possible explanations that are based off of our observed timescales.

It is reasonable to assume that the mechanisms responsible for melting superconductivity also play a role in its recovery. As mentioned above, we observe electronic and phononic timescales that contribute to the melting of superconductivity.

The first explanation is that pairs are reformed by the absorption of low-energy (acoustic) phonons, which can occur on nanosecond timescales. Indeed, this was used to explain the recovery of superconductivity after photoexcitation in the BCS superconductor MgB_2, which has gap sizes similar to the present material [50]. However, there are two main issues with this explanation: (1) Even in the case of MgB_2, some recombination is observed on a 100-ps timescale, and (2) it neglects the role of electronic and magnetic correlations that are known to play a key role in mediating iron-based superconductivity [31].

The second possibility is that the pairs are prevented from recombining because of the disruption to the correlations caused by the electronic redistribution. For example, direct

excitations can occur at different locations throughout the Brillouin zone. The natural pathways for relaxation may cause most holes to relax to the Γ point and most electrons to the M point in the Brillouin zone. This redistribution of particles modifies the correlations that are key to mediating iron-based superconductivity. Though it is difficult to narrow down the specific correlations that would be impacted, examining the changes that occur at higher excitation densities, where the changes are more apparent, may offer further insight. Thus, we turn to recent works that have identified a photoinduced metastable state in FST for clues. Properties of this metastable state include the renormalizations of the band structure and chalcogen positions that resemble the ground-state effects of increasing the Te concentration [11,13,25]. We therefore hypothesize that the photoinduced changes to the correlations are similar to those in higher Te concentrations.

At higher Te concentrations, the correlations favor double-stripe magnetism. Additionally, these magnetic correlations are known to compete with superconductivity [31]. We therefore hypothesize that the photoexcitation causes an orbital redistribution that favors double-stripe magnetic correlations, which act to melt superconductivity. Indeed, the sensitivity of superconductivity to the orbital redistribution is supported by electron diffraction work on $Ba(Fe_{1-x}Co_x)_2As_2$ that directly images the orbital configuration [51], as well as the strong polarization-dependent matrix elements of the SP observed in ARPES [2,3] and scanning tunneling microscopy [52] because they demonstrate the strong orbital dependence of the superconducting bands. Additionally, theoretical studies have demonstrated how the subtle balance among the band filling, the nearest and next-nearest superexchange interactions, and the Hund's coupling strength, which may be particularly sensitive to a pump-induced orbital redistribution, determine the magnetic ground state [33,34].

VI. CONCLUSION

In conclusion, we directly show, for the first time, the pump-induced changes to the electronic band structure of FST below T_c. Our observations show a reduction of two features that are directly associated with superconductivity, namely, the superconducting peak and gap. We observe changes on both electronic and picosecond timescales, and we find that they are metastable, lasting for more than 100 ps. Close examination of the initial changes to the band structure are indicative of nonequilibrium behavior that shows the filling of the superconducting gap occurring before the reduction of the SP. We hypothesize that the orbital fluctuations directly caused by the pump-induced electronic redistribution are linked to double-stripe magnetic correlations known to compete with superconductivity. A better theoretical understanding of the precise electronic excitations and relaxation pathways would be crucial in understanding the changes to the orbital occupancy that

results from the pump. Furthermore, experiments aimed at directly imaging the photoinduced orbital and magnetic changes, as well as tr-ARPES with high-energy resolution extending out to the edge of the Brillouin zone, would be needed in order to corroborate this picture and may ultimately yield clues to understanding the interactions that lead to iron-based superconductivity.

[1] Peng Zhang, Koichiro Yaji, Takahiro Hashimoto, Yuichi Ota, Takeshi Kondo, Kozo Okazaki, Zhijun Wang, Jinsheng Wen, G. D. Gu, Hong Ding, and Shik Shin, *Observation of Topological Superconductivity on the Surface of an Iron-Based Superconductor*, Science **360**, 182 (2018).

[2] J. D. Rameau, N. Zaki, G. D. Gu, P. D. Johnson, and M. Weinert, *Interplay of Paramagnetism and Topology in the* Fe-*Chalcogenide High-T_c Superconductors*, Phys. Rev. B **99**, 205117 (2019).

[3] Nader Zaki, Genda Gu, Alexei Tsvelik, Congjun Wu, and Peter D. Johnson, *Time-Reversal Symmetry Breaking in the* Fe-*Chalcogenide Superconductors*, Proc. Natl. Acad. Sci. U.S.A. **118**, e2007241118 (2021).

[4] Dongfei Wang, Lingyuan Kong, Peng Fan, Hui Chen, Shiyu Zhu, Wenyao Liu, Lu Cao, Yujie Sun, Shixuan Du, John Schneeloch, Ruidan Zhong, Genda Gu, Liang Fu, Hong Ding, and Hong-Jun Gao, *Evidence for Majorana Bound States in an Iron-Based Superconductor*, Science **362**, 333 (2018).

[5] Xianxin Wu, Suk Bum Chung, Chaoxing Liu, and Eun-Ah Kim, *Topological Orders Competing for the Dirac Surface State in* FeSeTe *Surfaces*, Phys. Rev. Res. **3**, 013066 (2021).

[6] Gang Xu, Biao Lian, Peizhe Tang, Xiao-Liang Qi, and Shou-Cheng Zhang, *Topological Superconductivity on the Surface of* Fe-*Based Superconductors*, Phys. Rev. Lett. **117**, 047001 (2016).

[7] Nathan J. McLaughlin, Hailong Wang, Mengqi Huang, Eric Lee-Wong, Lunhui Hu, Hanyi Lu, Gerald Q. Yan, Genda Gu, Congjun Wu, Yi-Zhuang You, and Chunhui Rita Du, *Strong Correlation between Superconductivity and Ferromagnetism in an* Fe-*Chalcogenide Superconductor*, Nano Lett. **21**, 7277 (2021).

[8] C. W. Luo, I. H. Wu, P. C. Cheng, J.-Y. Lin, K. H. Wu, T. M. Uen, J. Y. Juang, T. Kobayashi, D. A. Chareev, O. S. Volkova, and A. N. Vasiliev, *Quasiparticle Dynamics and Phonon Softening in* FeSe *Superconductors*, Phys. Rev. Lett. **108**, 257006 (2012).

[9] C. Bonavolontà, L. Parlato, G. P. Pepe, C. de Lisio, M. Valentino, E. Bellingeri, I. Pallecchi, M. Putti, and

C. Ferdeghini, *Ultrafast Quasiparticle Relaxation Dynamics in High Quality Epitaxial* $FeSe_{0.5}Te_{0.5}$ *Thin Films*, Supercond. Sci. Technol. **26**, 075018 (2013).

[10] Shuolong Yang, Jonathan A. Sobota, Dominik Leuenberger, Alexander F. Kemper, James J. Lee, Felix T. Schmitt, Wei Li, Rob G. Moore, Patrick S. Kirchmann, and Zhi-Xun Shen, *Thickness-Dependent Coherent Phonon Frequency in Ultrathin* $FeSe/SrTiO_3$ *Films*, Nano Lett. **15**, 4150 (2015).

[11] S. Gerber *et al.*, *Femtosecond Electron-Phonon Lock-in by Photoemission and X-Ray Free-Electron Laser*, Science **357**, 71 (2017).

[12] Takeshi Suzuki, Takashi Someya, Takahiro Hashimoto, Shoya Michimae, Mari Watanabe, Masami Fujisawa, Teruto Kanai, Nobuhisa Ishii, Jiro Itatani, Shigeru Kasahara, Yuji Matsuda, Takasada Shibauchi, Kozo Okazaki, and Shik Shin, *Photoinduced Possible Superconducting State with Long-Lived Disproportionate Band Filling in* FeSe, Communications in Physics **2**, 115 (2019).

[13] L. X. Yang, G. Rohde, Y. J. Chen, W. J. Shi, Z. K. Liu, F. Chen, Y. L. Chen, K. Rossnagel, and M. Bauer, *Experimental Evidence for a Metastable State in* $FeTe_{1x}Se_x$ *Following Coherent-Phonon Excitation*, J. Electron Spectrosc. Relat. Phenom. **250**, 147085 (2021).

[14] L. Perfetti, P. A. Loukakos, M. Lisowski, U. Bovensiepen, H. Eisaki, and M. Wolf, *Ultrafast Electron Relaxation in Superconducting* $Bi_2Sr_2CaCu_2O_{8+\delta}$ *by Time-Resolved Photoelectron Spectroscopy*, Phys. Rev. Lett. **99**, 197001 (2007).

[15] Rocia Cortés, L. Rettig, Y. Yoshida, H. Eisaki, Martin Wolf, and Uwe Bovensiepen, *Momentum-Resolved Ultrafast Electron Dynamics in Superconducting* $Bi_2Sr_2CaCu_2O_{8+\delta}$, Phys. Rev. Lett. **107**, 097002 (2011).

[16] Christopher L. Smallwood, James P. Hinton, Christopher Jozwiak, Wentao Zhang, Jake D. Koralek, Hiroshi Eisaki, Dung-Hai Lee, Joseph Orenstein, and Alessandra Lanzara, *Tracking Cooper Pairs in a Cuprate Superconductor by Ultrafast Angle-Resolved Photoemission*, Science **336**, 1137 (2012).

[17] S. Parham, H. Li, T. J. Nummy, J. A. Waugh, X. Q. Zhou, J. Griffith, J. Schneeloch, R. D. Zhong, G. D. Gu, and D. S. Dessau, *Ultrafast Gap Dynamics and Electronic Interactions in a Photoexcited Cuprate Superconductor*, Phys. Rev. X **7**, 041013 (2017).

[18] C. Piovera, Zhongkai Zhang, M. d'Astuto, A. Taleb-Ibrahimi, E. Papalazarou, M. Marsi, Z. Z. Li, H. Raffy, and L. Perfetti, *Quasiparticle Dynamics in High-Temperature Superconductors Far from Equilibrium: An Indication of Pairing Amplitude without Phase Coherence*, Phys. Rev. B **91**, 224509 (2015).

[19] J. D. Rameau, S. Freutel, L. Rettig, I. Avigo, M. Ligges, Y. Yoshida, H. Eisaki, J. Schneeloch, R. D. Zhong, Z. J. Xu *et al.*, *Photoinduced Changes in the Cuprate Electronic Structure Revealed by Femtosecond Time- and Angle-Resolved Photoemission*, Phys. Rev. B **89**, 115115 (2014).

[20] Tatiana Konstantinova, Jonathan D. Rameau, Alexander H. Reid, Omadillo Abdurazakov, Lijun Wu, Renkai Li, Xiaozhe Shen, Genda Gu, Yuan Huang, Laurenz Rettig *et al.*, *Nonequilibrium Electron and Lattice Dynamics of Strongly Correlated* $Bi_2Sr_2CaCu_2O_{8+\delta}$ *Single Crystals*, Sci. Adv. **4**, eaap7427 (2018).

[21] J. D. Rameau, S. Freutel, A. F. Kemper, Michael A. Sentef, J. K. Freericks, I. Avigo, M. Ligges, Laurenz Rettig, Y. Yoshida, H. Eisaki, J. Schneeloch, R. D. Zhong, Z. J. Xu, G. D. Gu, P. D. Johnson, and U. Bovensiepen, *Energy Dissipation from a Correlated System Driven out of Equilibrium*, Nat. Commun. **7**, 13761 (2016).

[22] F. Boschini, E. H. da Silva Neto, E. Razzoli, M. Zonno, S. Peli, R. P. Day, M. Michiardi, M. Schneider, B. Zwartsenberg, P. Nigge, R. D. Zhong, J. Schneeloch, G. D. Gu, S. Zhdanovich, A. K. Mills, G. Levy, D. J. Jones, C. Giannetti, and A. Damascelli, *Collapse of Superconductivity in Cuprates via Ultrafast Quenching of Phase Coherence*, Nat. Mater. **17**, 416 (2018).

[23] Georgi L. Dakovski, Tomasz Durakiewicz, Jian-Xin Zhu, Peter S. Riseborough, Genda Gu, Steve M. Gilbertson, Antoinette Taylor, and George Rodriguez, *Quasiparticle Dynamics across the Full Brillouin Zone of* $Bi_2Sr_2CaCu_2O_{8+\delta}$ *Traced with Ultrafast Time and Angle-Resolved Photoemission Spectroscopy*, Struct. Dyn. **2**, 054501 (2015).

[24] Federico Cilento, Giulia Manzoni, Andrea Sterzi, Simone Peli, Andrea Ronchi, Alberto Crepaldi, Fabio Boschini, Cephise Cacho, Richard Chapman, Emma Springate, Hiroshi Eisaki, Martin Greven, Mona Berciu, Alexander F. Kemper, Andrea Damascelli, Massimo Capone, Claudio Giannetti, and Fulvio Parmigiani, *Dynamics of Correlation-Frozen Antinodal Quasiparticles in Superconducting Cuprates*, Sci. Adv. **4**, eaar1998 (2018).

[25] Laura Fanfarillo, Damir Kopić, Andrea Sterzi, Giulia Manzoni, Alberto Crepaldi, Daniel T. Payne, Wibke Bronsch, Vladimir Tsurkan, Dorina Croitori, Joachim Deisenhofer, Fulvio Parmigiani, Massimo Capone, and Federico Cilento, *Photoinduced Long-Lived State in* $FeSe_{0.4}Te_{0.6}$, J. Electron Spectrosc. Relat. Phenom. **250**, 147090 (2021).

[26] Roman Mankowsky, Alaska Subedi, Michael Först, Simon O. Mariager, Matthieu Chollet, H. T. Lemke, Jeffrey S. Robinson, James M. Glownia, Michael P. Minitti, Alex Frano *et al.*, *Nonlinear Lattice Dynamics as a Basis for Enhanced Superconductivity in* $YBa_2Cu_3O_{6.5}$, Nature (London) **516**, 71 (2014).

[27] Matteo Mitrano, Alice Cantaluppi, Daniele Nicoletti, Stefan Kaiser, A. Perucchi, S. Lupi, P. Di Pietro, D. Pontiroli, M. Riccò, Stephen R. Clark *et al.*, *Possible Light-Induced Superconductivity in* K_3C_{60} *at High Temperature*, Nature (London) **530**, 461 (2016).

[28] R. Mankowsky, M. Fechner, M. Först, A. von Hoegen, J. Porras, T. Loew, G. L. Dakovski, M. Seaberg, S. Möller, G. Coslovich *et al.*, *Optically Induced Lattice Deformations, Electronic Structure Changes, and Enhanced Superconductivity in* $YBa_2Cu_3O_{6.48}$, Struct. Dyn. **4**, 044007 (2017).

[29] M. Budden, T. Gebert, M. Buzzi, G. Jotzu, E. Wang, T. Matsuyama, G. Meier, Y. Laplace, D. Pontiroli, M. Riccò *et al.*, *Evidence for Metastable Photo-Induced Superconductivity in* K_3C_{60}, Nat. Phys. **17**, 611 (2021).

[30] Yangmu Li, Nader Zaki, Vasile O. Garlea, Andrei T. Savici, David Fobes, Zhijun Xu, Fernando Camino, Cedomir Petrovic, Genda Gu, Peter D. Johnson, John M. Tranquada, and Igor A. Zaliznyak, *Electronic Properties of the Bulk and Surface States of* $Fe_{1+y}Te_{1x}Se_x$, Nat. Mater. **20**, 1221 (2021).

[31] John M. Tranquada, Guangyong Xu, and Igor A. Zaliznyak, *Magnetism and Superconductivity in* $Fe_{1+y}Te_{1-x}Se_x$, J. Phys. Condens. Matter **32**, 374003 (2020).

[32] Z. K. Liu, R.-H. He, D. H. Lu, M. Yi, Y. L. Chen, M. Hashimoto, R. G. Moore, S.-K. Mo, E. A. Nowadnick, J. Hu, T. J. Liu, Z. Q. Mao, T. P. Devereaux, Z. Hussain, and Z.-X. Shen, *Measurement of Coherent Polarons in the Strongly Coupled Antiferromagnetically Ordered Iron-Chalcogenide* $Fe_{1.02}Te$ *Using Angle-Resolved Photoemission Spectroscopy*, Phys. Rev. Lett. **110**, 037003 (2013).

[33] Wei-Guo Yin, Chi-Cheng Lee, and Wei Ku, *Unified Picture for Magnetic Correlations in Iron-Based Superconductors*, Phys. Rev. Lett. **105**, 107004 (2010).

[34] Wei-Guo Yin, Chi-Cheng Lee, and Wei Ku, *Magnetic Softness in Iron-Based Superconductors*, Supercond. Sci. Technol. **25**, 084007 (2012).

[35] P. D. Johnson, H.-B. Yang, J. D. Rameau, G. D. Gu, Z.-H. Pan, T. Valla, M. Weinert, and A. V. Fedorov, *Spin-Orbit Interactions and the Nematicity Observed in the Fe-Based Superconductors*, Phys. Rev. Lett. **114**, 167001 (2015).

[36] Himanshu Lohani, Tamaghna Hazra, Amit Ribak, Yuval Nitzav, Huixia Fu, Binghai Yan, Mohit Randeria, and Amit Kanigel, *Band Inversion and Topology of the Bulk Electronic Structure in* $FeSe_{0.45}Te_{0.55}$, Phys. Rev. B **101**, 245146 (2020).

[37] K. Okazaki, Y. Ito, Y. Ota, Y. Kotani, T. Shimojima, T. Kiss, S. Watanabe, C.-T. Chen, S. Niitaka, T. Hanaguri, H. Takagi, A. Chainani, and S. Shin, *Superconductivity in an Electron Band Just above the Fermi Level: Possible Route to BCS-BEC Superconductivity*, Sci. Rep. **4**, 4109 (2014).

[38] Y. Lubashevsky, E. Lahoud, K. Chashka, D. Podolsky, and A. Kanigel, *Shallow Pockets and Very Strong Coupling Superconductivity in* $FeSe_xTe_{1x}$, Nat. Phys. **8**, 309 (2012).

[39] Takahiro Hashimoto, Yuichi Ota, Akihiro Tsuzuki, Tsubaki Nagashima, Akiko Fukushima, Shigeru Kasahara, Yuji Matsuda, Kohei Matsuura, Yuta Mizukami, Takasada Shibauchi, Shik Shin, and Kozo Okazaki, *Bose-Einstein Condensation Superconductivity Induced by Disappearance of the Nematic State*, Sci. Adv. **6**, eabb9052 (2020).

[40] Shahar Rinott, K. B. Chashka, Amit Ribak, Emile D. L. Rienks, Amina Taleb-Ibrahimi, Patrick Le Fevre, François Bertran, Mohit Randeria, and Amit Kanigel, *Tuning across the BCS-BEC Crossover in the Multiband Superconductor* $Fe_{1+y}Se_xTe_{1-x}$: *An Angle-Resolved Photoemission Study*, Sci. Adv. **3**, e1602372 (2017).

[41] J. D. Rameau, H.-B. Yang, and P. D. Johnson, *Application of the Lucy–Richardson Deconvolution Procedure to High Resolution Photoemission Spectra*, J. Electron Spectrosc. Relat. Phenom. **181**, 35 (2010).

[42] See Supplemental Material at http://link.aps.org/supplemental/10.1103/PhysRevX.13.011001 for representative spectra following Lucy-Richardson deconvolution.

[43] Philip B. Allen, *Theory of Thermal Relaxation of Electrons in Metals*, Phys. Rev. Lett. **59**, 1460 (1987).

[44] Kazuki Isoyama, Naotaka Yoshikawa, Kota Katsumi, Jeremy Wong, Naoki Shikama, Yuki Sakishita, Fuyuki Nabeshima, Atsutaka Maeda, and Ryo Shimano, *Light-Induced Enhancement of Superconductivity in Iron-Based Superconductor* $FeSe_{0.5}Te_{0.5}$, Commun. Phys. **4**, 160 (2021).

[45] Xiaoxiang Xi, J. Hwang, C. Martin, D. B. Tanner, and G. L. Carr, *Far-Infrared Conductivity Measurements of Pair Breaking in Superconducting* $Nb_{0.5}Ti_{0.5}N$ *Thin Films Induced by an External Magnetic Field*, Phys. Rev. Lett. **105**, 257006 (2010).

[46] Yonah Lemonik and Aditi Mitra, *Quench Dynamics of Superconducting Fluctuations and Optical Conductivity in a Disordered System*, Phys. Rev. B **98**, 214514 (2018).

[47] M. R. Norman, M. Randeria, H. Ding, and J. C. Campuzano, *Phenomenology of the Low-Energy Spectral Function in High-T_C Superconductors*, Phys. Rev. B **57**, R11093 (1998).

[48] Hyok-Jon Kwon and Alan T. Dorsey, *Effect of Phase Fluctuations on the Single-Particle Properties of Underdoped Cuprates*, Phys. Rev. B **59**, 6438 (1999).

[49] M. Franz and A. J. Millis, *Phase Fluctuations and Spectral Properties of Underdoped Cuprates*, Phys. Rev. B **58**, 14572 (1998).

[50] J. Demsar, R. D. Averitt, A. J. Taylor, V. V. Kabanov, W. N. Kang, H. J. Kim, E. M. Choi, and S. I. Lee, *Pair-Breaking and Superconducting State Recovery Dynamics in* MgB_2, Phys. Rev. Lett. **91**, 267002 (2003).

[51] Chao Ma, Lijun Wu, Wei-Guo Yin, Huaixin Yang, Honglong Shi, Zhiwei Wang, Jianqi Li, C. C. Homes, and Yimei Zhu, *Strong Coupling of the Iron-Quadrupole and Anion-Dipole Polarizations in* $Ba(Fe_{1-x}Co_x)_2As_2$, Phys. Rev. Lett. **112**, 077001 (2014).

[52] Udai R. Singh, Seth C. White, Stefan Schmaus, Vladimir Tsurkan, Alois Loidl, Joachim Deisenhofer, and Peter Wahl, *Evidence for Orbital Order and Its Relation to Superconductivity in* $FeSe_{0.4}Te_{0.6}$, Sci. Adv. **1**, e1500206 (2015).